Low oxygen levels in earliest Triassic soils

Nathan D. Sheldon*
Gregory J. Retallack
Department of Geological Sciences, 1272, University of Oregon, Eugene, Oregon 97403, USA

ABSTRACT

An earliest Triassic methane postapocalyptic greenhouse following the Permian-Triassic (P-T) extinction event was proposed on the basis of evidence of deeply weathered paleosols at high latitudes with features of low-latitude soils, and low stomatal index values of seed fern leaves. Reexamination of distinctive phyllosilicates, unique to a single stratigraphic level, in paleosols located just above the isotopically defined Permian-Triassic boundary in Australia and Antarctica furnishes additional tests of this hypothesis. Illite is the dominant clay mineral in earliest Triassic paleosols from Antarctica, but the paleosols also contain conspicuous green nodules of coarsely crystalline berthierine. Examples from the geologic record and from experimental studies indicate that the formation of berthierine is restricted to reducing conditions. The occurrence of this unusual mineral in soils may indicate soil oxygen consumption by the influx of atmospheric methane to form carbon dioxide, which in turn warmed the earliest Triassic, giving rise to a postapocalyptic greenhouse.

Keywords: paleosols, berthierine, paleoclimate, Permian-Triassic, boundary.

INTRODUCTION

The Permian-Triassic life crisis was the greatest extinction in the history of life, variously attributed to an extraterrestrial impactor (Becker et al., 2001), Siberian Traps flood volcanism (Renne et al., 1995), oceanic anoxia (e.g., Hotinski et al., 2001), and food-web collapse (Wang et al., 1994). While the Permian-Triassic boundary has long been recognized as a catastrophic interval for marine life (Erwin, 1993), numerous lines of evidence, including a global fungal spike (Eshet et al., 1995), global coal gap (Retallack et al., 1996), and significant diversity loss of fossil plants (Looy et al., 1999) and animals (Smith and Ward, 2001), point to similar decimation of terrestrial biota. Retallack (1999) and Retallack and Krull (1999) suggested that the earliest Triassic was marked by a postapocalyptic greenhouse: an abrupt shift to warmer temperatures, and to oligotrophic, low-productivity ecosystems at high latitudes. Krull et al. (2000) and Krull and Retallack (2000) used $\delta^{13}C_{organic}$ evidence to suggest a high-latitude CH_4 (methane) release in the earliest Triassic, and de Wit et al. (2002) emphasized that $\delta^{13}C_{organic}$ changes are consistent with multiple methane dissociation events. Carbon cycle modeling by Berner (2002) indicates that the $\delta^{13}C$ isotopic excursion across the Permian-Triassic boundary is best explained by the introduction of methane to the atmosphere. The release could come from either marine methane clathrates or from extensive high-latitude permafrost clathrates (Retallack and Krull, 1999; Krull et al., 2000). An initial perturbation of marine or permafrost clathrates from any of these mechanisms, or some combination of them, would lead to increased atmospheric CH_4 and its oxidation product CO_2, which could in turn lead to further clathrate melting as a positive feedback for the global climate system. An abrupt rise in CO_2 is also revealed by an abrupt decline in the stomatal index of earliest Triassic seed ferns (Retallack, 2001). Such an event could dramatically change the redox conditions of the atmosphere and the soil-atmosphere interface because large amounts of oxygen would be consumed in oxidizing the CH_4 to CO_2.

With these ideas in mind we analyzed phyllosilicates and carbonates from paleosols, stratigraphically just above the isotopically located Permian-Triassic boundary in Australia and Antarctica. At Graphite Peak, Mount Crean, and Allan Hills in Antarctica (Retallack and Krull, 1999), the Dolores pedotype has prominent green phyllosilicate nodules, which are unknown from paleosols at any other Permian or younger Triassic level in the sections. The sideritic Wybung pedotype in the Australia sections at Wybung Head and Coalcliff is also confined to the boundary interval (Retallack, 1999). X-ray diffraction (XRD) on the clay fraction (<2 μm) of all the paleosols showed a strong 7 Å (*d*-spacing) peak as in berthierine, but also a 14 Å peak as in chlorite, barely above background (Fig. 1). Because berthierine is unusual and chlorite common, the green mineral was originally designated chlorite (Retallack and Krull, 1999). Berthierine is an iron-aluminum 1:1-type layer silicate of the serpentine group that may be mistaken for chamosite (Fe-chlorite;

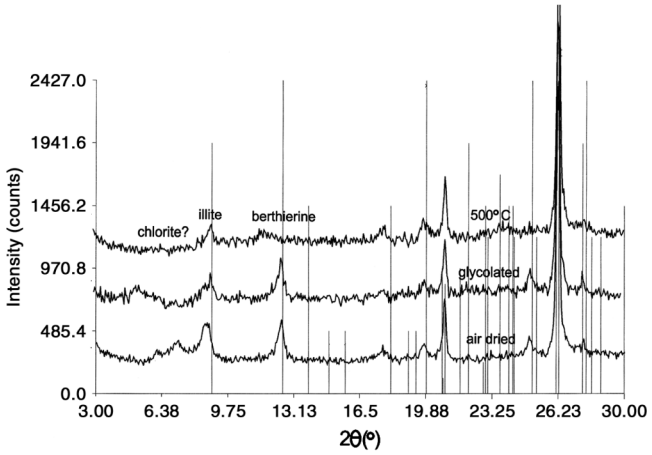

Figure 1. X-ray diffraction trace of Antarctic earliest Triassic paleosol obtained with Cu-kα radiation. Sample A-2058 is from Dolores pedotype in Antarctica (Retallack and Krull, 1999). Prominent 7 and 10 Å peaks represent illite and berthierine, dominant phyllosilicates in Antarctic samples. Subdued 14 Å peak indistinguishable from background is consistent with limited conversion of berthierine to chlorite. Berthierine, present in low-temperature analyses, is lost at 500 °C due to oxidation.

*E-mail: nsheldon@darkwing.uoregon.edu.

© 2002 Geological Society of America. For permission to copy, contact Copyright Permissions, GSA, or editing@geosociety.org.

Brindley, 1982). Berthierine has been found in a number of chemically reducing depositional settings, including marine mudstones (Ahn and Peacor, 1985), ironstones (Taylor and Curtis, 1995), as ooids or pisoids (Hornibrook and Longstaffe, 1996), or in sulfide deposits (Jiang et al., 1992), and it is rarely found as a soil mineral (Fritz and Toth, 1997; Taylor, 1990; Kodama and Foscolos, 1981). Berthierine is an indicator of chemically reducing conditions (Fritz and Toth, 1997; Taylor and Curtis, 1995) where sulfide and bicarbonate activity is low because pyrite and siderite, respectively, form instead if those species are present at sufficiently high levels. Sawicki et al. (1995) described a biofilm with protoferrihydrite forming on one side and siderite forming on the other. This suggests that biomineralization can play an important role in the fabrication of ferrous iron minerals. Given that siderite is present in the Australian paleosol, biomineralization may have been important; however, little is known about the role of microbes in berthierine formation. The object of this study was to use a combination of electron probe microanalysis (EPMA) and scanning electron microscopy (SEM) to study clay minerals in the earliest Triassic paleosols from Antarctica and Australia to differentiate between chlorite and berthierine and to examine their relevance to paleoatmospheric conditions using a simple thermodynamic model.

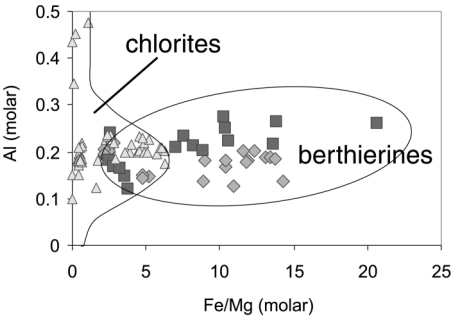

Figure 2. Plot of molar ratio of iron to magnesium versus aluminum from microprobe analyses, using data from electron beam microprobe analysis of earliest Triassic samples from Antarctica (Retallack and Krull, 1999; Krull and Retallack, 2000) and Australia (Retallack, 1999). Berthierines from this study are diamonds, berthierines from previous studies (Brindley, 1982; Hornibrook and Longstaffe, 1996) are squares, and triangles are chlorite analyses from various sources (Bailey, 1988; Cathelineau and Nieva, 1985; Abad-Ortega and Nieto, 1995). There is some overlap between berthierine and chlorite fields, indicating partial conversion of berthierine to chlorite. While berthierine typically has 15%–25% alumina by weight, chlorite may have significantly more or less alumina. Chlorite may also substitute significant amount of manganese for iron or magnesium because of its crystal structure, whereas berthierine typically contains very modest amounts of metals other than iron and magnesium.

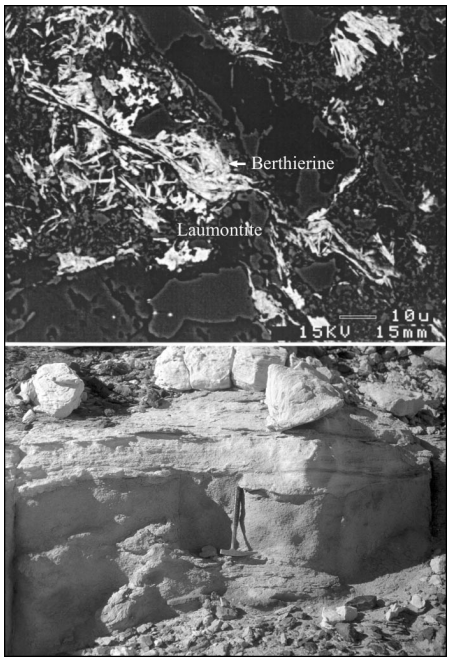

Figure 3. Top: Scanning electron microscope image of berthierine from earliest Triassic paleosol, Graphite Peak, Antarctica, shows euhedral, authigenic, interstitial form, and lack of evidence for alteration either to siderite or from siderite. This indicates that siderite was likely never present and that pore fluid from which berthierine crystallized had insufficient bicarbonate to precipitate siderite. Bottom: Green bench of Dolores paleosols forms distinctive stratigraphic and topographic level between cliffs of Permian coal measures below and Triassic quartz sandstones above (central Allan Hills, Antarctica).

METHODS

Polished thin sections of six samples were used for EPMA, and two of those same samples were used for SEM analysis. Table DR-1[1] summarizes sample characteristics. All six samples were examined petrographically and with XRD in addition to EPMA and SEM analysis.

To differentiate between chlorite and berthierine, selected grains were analyzed for major element oxides using quantitative EPMA with an acceleration voltage of 15 keV and a regulated beam current of 10 nA. All backscatter images were obtained using an acceleration voltage of 15 keV and an unregulated beam current of ~2.5 ± 0.1 nA. The image capture time was 40 s. EPMA count times were variable according to the element, ranging from 10 s (Na) to 30 s (Mn); most elements were counted for 20 s.

RESULTS

SEM-EDS (energy-dispersive) spectra with iron, silicon, and aluminum peaks were selected for imaging. Most of these spectra also included a small, though significant, peak at magnesium. Among the other minerals present were smectite, illite, titanite, quartz, hematite, and rare feldspar grains. Australian samples also had kaolinite and siderite, while the Antarctic samples lacked siderite and had little or no kaolinite. Common features of the berthierines from the literature and the grains from this study are elongation of the grains and intergrowth of the crystals with others (Fig. 2). Figure 2 also shows that the grains in this study are authigenic because there are no metamorphic features such as planar fracturing or dissolution (Retallack and Krinsley, 1993); nor is there rounding, ferruginization, or other evidence of transport.

Our analytical data for iron-bearing clays (Table DR-2; see footnote 1) can be compared with previous berthierine analyses of Brindley (1982), Toth and Fritz (1997), and Hornibrook and Longstaffe (1996) in Table DR-3 (see footnote 1). Some of the grains analyzed in this study are iron poor and magnesium rich relative to most of the analyses presented by Brindley (1982) and to the data of Toth and Fritz (1997), but are very similar compositionally to other berthierines of Brindley (1982) and Hornibrook and Longstaffe (1996) (Fig. 3). Low oxide totals of Tables DR-2 and DR-3 represent loss of water, because both chlorite and berthierine are hydrous minerals.

As noted by Brindley (1982), the presence of a small amount of clinochlore (Mg-chlorite) can obfuscate identification of berthierine, and that may be the case here. The chemical data from Graphite Peak and a few of the Allan Hills samples plot within the zone where the berthierine and chlorite fields overlap (Fig. 3), so they may represent a dominantly berthierine mineralogy that is diluted by partial admixture with magnesium-rich chlorite, probably due to the conversion of berthierine to chlorite by low-temperature metamorphism. Most of the Australian berthierines plot well outside the chlorite field and show significant overlap with previous berthierine analyses (Fig. 3). Siderite was only found in the Australian samples from Coal Cliff and Wybung Head, and may be the end product of a goethite-berthierine-siderite paragenetic sequence (Bhattacharyya, 1983), indicating prolonged reducing conditions. Typical compositions of Coal Cliff siderites are summarized in Table DR-4 (see footnote 1).

DISCUSSION

Soils form in direct contact with the atmosphere; atmospheric and soil gases exchange

[1]GSA Data Repository item 2002109, Tables DR-1 to DR-5, sample descriptions, microprobe data, and thermodynamic data, is available from Documents Secretary, GSA, P.O. Box 9140, Boulder, CO 80301-9140, editing@geosociety.org, or at www.geosociety.org/pubs/ft2002.htm.

freely at the soil-atmosphere interface. Significant changes to atmospheric gas compositions, drive changes in soil gas compositions both directly (diffusion processes) and indirectly (changing soil respiration processes). A methane dissociation event would change soil gas chemistry both by the diffusion of methane into the soil and potentially by lowering atmospheric oxygen levels as methane oxidized in the atmosphere. Although soils may have significantly more methane or carbon dioxide than the atmosphere, no process exists for the partial pressures of those gases to be lower than those of the atmosphere. Therefore, high atmospheric methane concentrations translate to high soil methane concentrations.

While berthierine formation requires only chemically reducing conditions, there are few documented occurrences (Fritz and Toth, 1997; Taylor, 1990; Kodama and Foscolos, 1981), suggesting that special conditions such as elevated soil methane levels may be necessary to facilitate its formation in soils. Two possible origins for berthierine have been suggested: the reaction of kaolinite and goethite or hematite (essentially dehydrated goethite) in the presence of magnesium (Bhattacharyya, 1983), or from the breakdown of oxides and primary clay minerals such as smectites (Taylor and Curtis, 1995). Both reaction pathways likely played a role in the formation of berthierine in Australian and Antarctic soils of the earliest Triassic. The Australian paleosol is kaolinite rich and smectite poor, while the Antarctic paleosols are kaolinite free but smectite and illite rich. Owing to uncertainties in the chemical formulae and thermodynamic properties of smectites and illites, it is most illustrative to consider the chemistry of the Australian paleosol. All thermodynamic data are taken from the SOLTHERM database, the composition of which was explained in Palandri and Reed (2001). A reaction for the equilibrium between berthierine and kaolinite and hematite can be written as:

$$Al_2Si_2O_5(OH)_{4\ kaol} + Fe_2O_{3\ hem} = Fe_2Al_2SiO_5(OH)_{4\ bert} + SiO_{2(aq)} + \tfrac{1}{2}O_{2(g)}, \quad (1)$$

with log $K = -38.948$ at 25 °C (individual reactions and K values are in Table DR-5; see footnote 1). A simple reaction, probably correct for most soils, for the oxidation of methane to form carbon dioxide is given by:

$$\tfrac{1}{4}CH_{4(g)} + \tfrac{1}{2}O_{2(g)} = \tfrac{1}{4}CO_{2(g)} + \tfrac{1}{2}H_2O_{(aq)}, \quad (2)$$

with log $K = 37.275$ at 25 °C. Each mole of methane added thus consumes 2 mol of oxygen gas. Combining reactions 1 and 2, the total reaction can be written for soil solutions:

$$Al_2Si_2O_5(OH)_{4\ ka} + Fe_2O_{3\ hem} + \tfrac{1}{4}CH_4 = Fe_2Al_2SiO_5(OH)_{4\ bert} + SiO_{2(aq)} + \tfrac{1}{2}H_2O_{(aq)} + \tfrac{1}{4}CO_{2(g)}, \quad (3)$$

with log $K = -1.673$ at 25 °C. This relationship can be used to examine the balance between methane and carbon dioxide using a couple of assumptions. First, the activities of pure minerals and of water are taken to be unity. Second, if the total pressure of the system is one bar, as in the present atmosphere, fugacity coefficients are also unity, so gas fugacities can be expressed as partial pressures (p). This gives rise to the following expression relating the pressures of methane and carbon dioxide:

$$K = 10^{-1.673} = p^{\frac{1}{4}}(CO_2)/p^{\frac{1}{4}}(CH_4). \quad (4)$$

From Lechatelier's Principle, addition of methane to Australian soils from the atmosphere would drive the formation of carbon dioxide. The present atmosphere has ~1.6 ppmv methane (Kasting et al., 2001). Strong evidence has been presented for methane clathrate dissociation as the mechanism of warming during the latest Paleocene thermal maximum, when an estimated 500–1000 Gt of methane were added to the atmosphere (Katz et al., 1999). There is at present ~615 Gt of total carbon in the atmosphere (de Wit et al., 2002), mostly as carbon dioxide. Given the significantly larger isotopic shift across the Permian-Triassic boundary (e.g., Krull and Retallack, 2000), the magnitude of methane release may have also been significantly larger. To be conservative, consider methane addition of 100 times present atmospheric levels (160 ppmv, equivalent to adding <300 Gt of methane). At equilibrium and assuming quartz saturation, this methane addition would be balanced by 0.021 bar of CO_2, or ~60 times present atmospheric levels. Thus, a relatively small addition of methane to the atmosphere would result in soil carbon dioxide concentrations comparable to tropical ecosystems (Brook et al., 1983). Less conservative scenarios for methane addition would drive the partial pressure of carbon dioxide even higher.

Reconsidering equation 1, it is also possible to quantitatively assess the partial pressure of oxygen making similar assumptions to those used in applying equation 4,

$$K = 10^{-38.948} = [a(SiO_2)][p^2(O_2)], \quad (5)$$

where a is activity. Assuming quartz saturation, equation 5 gives $pO_2 = 3.54 \times 10^{-18}$ bar. The present atmosphere has ~0.2 bar of O_2, so the presence of an assemblage of berthierine, hematite, and kaolinite in earliest Triassic soils suggests severe soil dysoxia. If the source of the dysoxia necessary to facilitate berthierine formation is increased atmospheric methane, this result is consistent with Dickens' (2001) suggestion that the most important consequence of methane release may be oxygen depletion rather than atmospheric warming. Berner's (2002) carbon cycle model also predicts lowered global atmospheric pO_2 relative to present values. While 25 °C is almost certainly too warm for the earliest Triassic, lowering the temperature to 0–10 °C, Retallack's (1999) reconstructed mean annual temperature, has the effect of leading to even lower estimates of pO_2 and higher pCO_2 (Fig. 4). Most natural waters have aqueous silica contents of at least quartz saturation ($10^{-4.047}$ at 25 °C), and higher silica values (e.g., chalcedony saturation; $10^{-3.728}$ at 25 °C) would result in significantly higher pCO_2 (Fig. 4). The higher temperature and lower silica estimates are used because thermodynamic properties of most minerals are measured rather than extrapolated for 25 °C, and because they represent the most conservative estimates. Given that the methane release was possibly 3–14 times larger and the temperature significantly lower than 25 °C, carbon dioxide levels of 60 times present levels calculated previously are probably on the low end of the range of possible values. If methane additions recurred over a longer time frame (rather than in the single pulse modeled here), as suggested by de Wit et al. (2002), then the higher values in Figure 4 might represent transient peaks (methane's residence time in the atmosphere is only ~10 yr [Berner, 2002]) during the

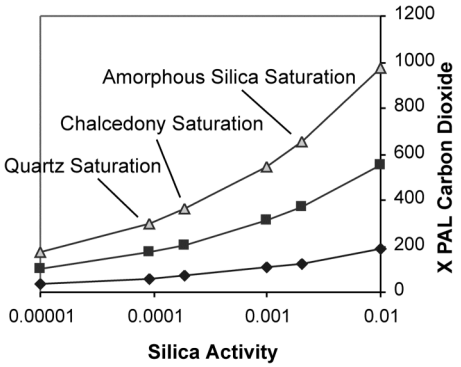

Figure 4. Comparison of silica activity to predicted CO_2 for various temperatures. Predicted CO_2 values vary as function of silica activity and of temperature. Arrows for different silica polymorphs reflect their saturation values at 25 °C (diamonds). Squares (15 °C) and triangles (10 °C) depict effects of changing temperature. At aqueous silica activities near quartz or chalcedony, saturation temperature has significantly smaller effect on predicted soil CO_2 values than for unrealistically high silica values on right of figure. PAL—present atmospheric levels.

event rather than the amount of CO_2 present for a prolonged time.

Earliest Triassic paleosols in Australia and Antarctica are gleyed (waterlogged) Inceptisols. Addition of methane to the atmosphere would have two effects: (1) soil oxygen would be consumed by the oxidation of methane to form carbon dioxide, leading to nearly anoxic conditions; (2) soil carbon dioxide levels at high latitudes would increase to levels consistent with the tropics. Calculations of soil gas chemistry here are consistent with Retallack's (1999) description of Early Triassic paleosols that had undergone chemical weathering inconsistent with their high paleolatitude and consistent with subtropical conditions. Severe changes in soil gas chemistry resulting from rapid atmospheric changes would likely be the most devastating in waterlogged soils in Australia and Antarctica, where oxygen levels would have already been low. Dysoxia and hypercapnia (high pCO_2) in the soils would likely decimate most nonbacterial biota, possibly leading to a destabilization of the landscape that could result in increased terrigenous sediment flux (Ward et al., 2000) to shallow shelf areas, perhaps exacerbating existing hypercapnia and dysoxia (Hotinski et al., 2001; Berner, 2002). Dysoxia would be especially critical in wetland soils, where extinctions were profound enough to cause a prolonged coal gap (Retallack et al., 1996). Whether soils at other latitudes underwent dysoxia and hypercapnia is an open question, but high-latitude, lowland ecosystems appear to have been choked by a methane-derived postapocalyptic greenhouse.

ACKNOWLEDGMENTS

Support for the field work was provided by National Science Foundation grant OPP-9315228. We thank Cliff Ambers (X-ray diffraction), Lori Suskin (sample preparation), and Michael Shaffer (electron probe microanalysis, scanning electron microscope) for logistical support. This manuscript benefited from comments on an earlier version by Paul Schroeder and an anonymous reviewer.

REFERENCES CITED

Abad-Ortega, M., and Nieto, F., 1995, Extension and closure of the compositional gap between Mn- and Mg-rich chlorites toward Fe-rich compositions: European Journal of Mineralogy, v. 7, p. 363–367.

Ahn, J.H., and Peacor, D.R., 1985, Transmission electron microscopic study of diagenetic chlorite in Gulf Coast argillaceous sediments: Clays and Clay Minerals, v. 33, p. 228–236.

Bailey, S.W., 1988, Chlorites: Structures and crystal chemistry, *in* Bailey, S.W., ed., Hydrous phyllosilicates (exclusive of micas): Mineralogical Society of America Reviews in Mineralogy, v. 19, p. 346–403.

Becker, L., Poreda, R.J., Hunt, A.G., Bunch, T.E., and Rampino, M., 2001, Impact event at the Permian-Triassic boundary: Evidence from extraterrestrial noble gases in fullerenes: Science, v. 291, p. 1530–1533.

Berner, R.A., 2002, Examination of hypotheses for the Permo-Triassic boundary extinction by carbon cycle modeling: National Academy of Sciences Proceedings, v. 99, p. 4172–4177.

Bhattacharyya, D.P., 1983, Origin of berthierine in ironstones: Clay and Clay Minerals, v. 31, p. 173–182.

Brindley, G.W., 1982, Chemical compositions of berthierines: A review: Clays and Clay Minerals, v. 30, p. 153–155.

Brook, G.A., Folkoff, M.E., and Box, E.O., 1983, A world model of carbon dioxide: Earth Surface Processes and Landforms, v. 8, p. 79–88.

Cathelineau, M., and Nieva, D., 1985, A chlorite solid solution geothermometer for the Los Azufres (Mexico) geothermal system: Contributions to Mineralogy and Petrology, v. 91, p. 235–244.

de Wit, M.J., Ghosh, J.G., de Villiers, S., Rakotosolofo, N., Alexander, J., Tripathi, A., and Looy, C., 2002, Multiple organic carbon isotope reversals across the Permo-Triassic boundary of terrestrial Gondwana sequences: Clues to extinction patterns and delayed ecosystem recovery: Journal of Geology, v. 110, p. 227–246.

Dickens, G., 2001, On the fate of past gas: What happens to methane released from a bacterially mediated gas hydrate capacitor: Geochemistry, Geophysics, Geosystems, v. 2, paper no. 2000GC000131.

Erwin, D.H., 1993, The great Paleozoic crisis: Life and death in the Permian: New York, Columbia University Press, 327 p.

Eshet, Y., Rampino, M.R., and Visscher, H., 1995, Fungal event and palynological record of ecological crisis across the Permian-Triassic boundary: Geology, v. 23, p. 967–970.

Fritz, S.J., and Toth, T.A., 1997, An Fe-berthierine from a Cretaceous laterite: Part II, estimation of Eh, pH and pCO_2 conditions of formation: Clays and Clay Minerals, v. 45, p. 580–586.

Hornibrook, E.R.C., and Longstaffe, F.J., 1996, Berthierine from the Lower Cretaceous Clearwater Formation, Alberta, Canada: Clays and Clay Minerals, v. 44, p. 1–21.

Hotinski, R.M., Bice, K.L., Kump, L.R., Najjar, R.G., and Arthur, M.A., 2001, Ocean stagnation and end-Permian anoxia: Geology, v. 29, p. 7–10.

Jiang, Wei-The, Peacor, D.R., and Slack, J.F., 1992, Microstructures, mixed layering, and polymorphism of chlorite and retrograde berthierine in the Kidd Creek massive sulfide deposit, Ontario: Clay and Clay Minerals, v. 40, p. 501–514.

Kasting, J.F., Pavlov, A.A., and Seifert, J.L., 2001, A coupled ecosystem-climate for predicting the methane concentration in the Archean atmosphere: Origins of Life and Evolution of the Biosphere, v. 31, p. 271–285.

Katz, M.E., Pak, D.K., Dickens, G.R., and Miller, K.G., 1999, The source and fate of massive carbon input during the latest Paleocene thermal maximum: Science, v. 286, p. 1531–1533.

Kodama, H., and Foscolos, A.E., 1981, Occurrence of berthierine in Canadian Arctic desert soils: Canadian Mineralogist, v. 19, p. 279–283.

Krull, E.S., and Retallack, G.J., 2000, $\delta^{13}C$ depth profiles from paleosols across the Permian-Triassic boundary: Evidence for methane release: Geological Society of America Bulletin, v. 112, p. 1459–1472.

Krull, E.S., Retallack, G.J., Campbell, H.J., and Lyon, G.L., 2000, $\delta^{13}C_{org}$ chemostratigraphy of the Permian-Triassic boundary in the Maitai Group, New Zealand: Evidence for high-latitudinal methane release: New Zealand Journal of Geology and Geophysics, v. 43, p. 21–32.

Looy, C.V., Brugman, W.A., Dilcher, D.L., and Visscher, H., 1999, The delayed resurgence of equatorial forests after the Permian-Triassic ecologic crisis: National Academy of Sciences Proceedings v. 96, p. 13 857–13 862.

Palandri, J.L., and Reed, M.H., 2001, Reconstruction of in situ composition of sedimentary formation waters: Geochimica et Cosmochimica Acta, v. 65, p. 1741–1767.

Renne, P.R., Zichao, Z., Richards, M.A., Black, M.T., and Basu, A.R., 1995, Synchrony and causal relations between Permian-Triassic boundary crises and Siberian flood basalt volcanism: Science, v. 269, p. 1413–1416.

Retallack, G.J., 1999, Postapocalyptic greenhouse paleoclimate revealed by earliest Triassic paleosols in the Sydney Basin, Australia: Geological Society of America Bulletin, v. 111, p. 52–70.

Retallack, G.J., 2001, A 300-million-year record of atmospheric carbon dioxide from fossil plant cuticles: Nature, v. 411, p. 287–290.

Retallack, G.J., and Krinsley, D.H., 1993, Metamorphic alteration of a Precambrian (2.2 Ga) paleosol from South Africa revealed by backscattered electron imaging: Precambrian Research, v. 63, p. 27–41.

Retallack, G.J., and Krull, E.S., 1999, Landscape ecological shift at the Permian-Triassic boundary in Antarctica: Australian Journal of Earth Sciences, v. 46, p. 785–812.

Retallack, G.J., Veevers, J.J., and Morante, R., 1996, Global Early Triassic coal gap between Permo-Triassic extinction and Middle Triassic recovery of swamp floras: Geological Society of America Bulletin, v. 108, p. 195–207.

Sawicki, J.A., Brown, D.A., and Beveridge, T.J., 1995, Microbial precipitation of siderite and protoferrihydrite in a biofilm: Canadian Mineralogist, v. 33, p. 1–6.

Smith, R.M.H., and Ward, P.D., 2001, Pattern of vertebrate extinctions across an event bed at the Permian-Triassic boundary in the Karoo Basin of South Africa: Geology, v. 29, p. 1147–1150.

Taylor, K.G., 1990, Berthierine from the non-marine Wealden (Early Cretaceous) sediments of southeast England: Clay Minerals, v. 25, p. 391–399.

Taylor, K.G., and Curtis, C.D., 1995, Stability and facies association of early diagenetic mineral assemblages: An example from a Jurassic ironstone-mudstone succession, U.K.: Journal of Sedimentary Research, Section A: Sedimentary Petrology and Processes, v. 65, p. 358–368.

Toth, T.A., and Fritz, S.J., 1997, An Fe-berthierine from a Cretaceous laterite: Part I, characterization: Clays and Clay Minerals, v. 45, p. 564–579.

Wang, K., Geldsetzer, H.H.J., and Krouse, H.R., 1994, Permian-Triassic extinction: Organic $\delta^{13}C$ evidence from British Columbia, Canada: Geology, v. 22, p. 580–584.

Ward, P.D., Montgomery, D.R., and Smith, R., 2000, Altered river morphology in South Africa related to the Permian-Triassic extinction: Science, v. 289, p. 740–743.

Manuscript received March 7, 2002
Revised manuscript received June 18, 2002
Manuscript accepted June 21, 2002

Printed in USA